Optimum Design of Thick Laminated Anisotropic Plates via Frequency Regulation. A BEM Approach

J. T. Katsikadelis and N. G. Babouskos

Abstract The optimum design of a thick laminated anisotropic plate in order to regulate its dynamic response is studied. The optimization problem consists in establishing the ply orientation of each layer for which the fundamental frequency is maximized, minimized or forced to reach a prescribed value. The evaluation of the objective function requires the solution of the dynamic bending problem of a thick laminated plate which is solved using the Analog Equation Method (AEM) in conjunction with the Boundary Element Method (BEM). A nonlinear optimization problem is formulated and the optimum solution is obtained through the sequential quadratic programming algorithm. Several plate optimization problems have been studied giving realistic and meaningful optimum designs.

1 Introduction

Laminated plates made of various layers of anisotropic materials exhibit certain significant advantages over singled layer plates. For this reason they are extensively used in various engineering structures, like buildings, ship, aircrafts and space structures. Laminated plates give the designers the opportunity to optimize their response according to structural requirements. By changing the material principal directions of each layer, the number of the layers, their thickness or their sequence we can minimize the weight of the structure, maximize the buckling load, regulate natural frequencies or minimize the deflection of the plate.

J. T. Katsikadelis (✉) · N. G. Babouskos
School of Civil Engineering, National Technical University of Athens
Zografou Campus, Athens 15773, Greece
e-mail: jkats@central.ntua.gr

H. Altenbach et al. (eds.), *Advances in Mechanics of Materials and Structural Analysis*, Advanced Structured Materials 80,
https://doi.org/10.1007/978-3-319-70563-7_10

Frequency regulation is of great importance in structures under dynamic excitation. By regulating (minimizing, maximizing or specifying) the fundamental or higher order natural frequencies, we can avoid the destructive consequences of various dynamic phenomena, like resonance and flutter instability.

The frequency optimization of thin and thick laminated plates has been studied by many researchers. Most of them investigate frequency optimization by maximizing the fundamental frequency using as design variables the fiber orientation and the thickness of each layer. Narita [1, 2], Apalak et al. [3] and Ghashochi [4] study frequency maximization of thin laminated plates using the Finite Element Method (FEM). Houmat [5] study frequency maximization assuming that fiber orientation may be position dependent within a layer of a thin plate.

Many researchers have shown that shear effects cannot be neglected even in thin laminated anisotropic plates, which are made of modern materials with increased ratio of Young to shear modulus [6]. Fares et al. [7] investigate optimal design of laminated plates using various plate theories. They optimize the dynamic response of the plate using as design variables the fiber orientation and the thickness of the layers. They concluded that Mindlin plate theory give results close to higher order theories in case of moderate thick laminated plates. Frequency optimization of Mindlin laminated plates has been studied by many researchers using FEM and gradient optimization methods [8–10]. Some researchers minimize the weight of the plate under a frequency constraint using as design variables the fiber orientation of each layer [11–13]. Modern evolutionary optimization methods have been also used in frequency optimization of thick laminated plates [14–16].

In this paper we consider the problem of frequency regulation of a thick laminated plate made of various orthotropic layers. The plate may have arbitrary geometry and is subjected to any type of boundary conditions. The optimization problem consists in determining the angle of the material principal direction of each layer (ply orientation) for which the plate fundamental frequency is optimized, i.e., it becomes minimum, maximum or reaches certain specified value between the extrema. The optimization problem is subjected to upper and lower bounds on ply orientation. The evaluation of the objective function (fundamental frequency) requires the solution of the free vibration problem of an anisotropic thick plate, which is described by a system of three coupled hyperbolic partial differential equations (PDE) of second order. Following the principle of the analog equation [17], the original system of equations is substituted by three uncoupled quasi-static Poisson's equation under fictitious loads. The Poisson's equations are solved using the conventional BEM [18] with constant boundary elements and linear triangular elements for domain discretization. The optimization problem is solved using sequential quadratic programming algorithm by a ready to use Matlab function. Several optimization problems for plates of various shapes and boundary conditions have been analyzed, yielding thus realistic and meaningful optimum designs.

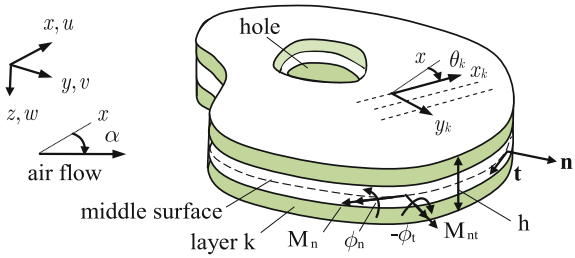

Fig. 1 Laminated thick plate

2 Statement of the Problem

2.1 Optimization Problem

We consider a thick elastic plate made of L orthotropic layers of uniform thickness occupying the two-dimensional multiply connected domain Ω in the xy-plane with the boundary $\Gamma = \cup_{i=0}^{i=K} \Gamma_i$ (Fig. 1). The nonintersecting curves $\Gamma_i \quad (i = 0, 1, 2, \ldots, K)$ may be piecewise smooth. The principal axes $(x_k^{,} y_k^{)} \quad (k = 1, 2, \ldots, L)$ of the k-lamina may be inclined at an angle θ_k with respect to global coordinate system (Fig. 1). The plate may be simply supported, clamped or free along the boundary. The objective function of the problem is the fundamental frequency, which is obtained from the solution of the free vibration problem in absence of damping.

The optimization problem consists in determining the angles $\theta_k \quad (k = 1, 2, \ldots, L)$ for which the fundamental frequency becomes maximum or minimum or takes a certain specified value between them. Thus, the evaluation of the objective function requires the solution of the dynamic bending problem of an anisotropic thick plate.

2.2 The Equation of Motion of a Thick Laminated Anisotropic Plate

The Mindlin plate theory [19] is adopted to approximate the response of the thick plate. According to this theory the displacement field is given as

$$u(x, y, z) = z\phi_x(x, y), v(x, y, z) = z\phi_y(x, y), \quad w(x, y, z) = w(x, y) \tag{1a, b, c}$$

where w is the transverse deflection of the middle surface of the plate and ϕ_x, ϕ_y its rotations about y and x axis, respectively.

The constitutive equations of the $k = 1, 2, \ldots, L$ layer, which is made of an orthotropic material, are given as

$$\begin{Bmatrix} \sigma_x \\ \sigma_y \\ \tau_{xy} \end{Bmatrix}^k = \begin{bmatrix} C_{11} & C_{12} & C_{16} \\ C_{12} & C_{22} & C_{26} \\ C_{16} & C_{26} & C_{66} \end{bmatrix}^k \begin{Bmatrix} z\phi_{x,x} \\ z\phi_{y,y} \\ z(\phi_{x,y} + \phi_{y,x}) \end{Bmatrix} \tag{2}$$

$$\begin{Bmatrix} \tau_{xz} \\ \tau_{yz} \end{Bmatrix}^k = \begin{bmatrix} C_{55} & C_{45} \\ C_{45} & C_{44} \end{bmatrix}^k \begin{Bmatrix} \phi_x + w,_x \\ \phi_y + w,_y \end{Bmatrix} \tag{3}$$

where C_{ij} are the elastic constants of the orthotropic material as transformed from the material axes (x_k, y_k) to the global axes (x, y) [17, 20]. Thus, the stress resultants are

$$\begin{Bmatrix} M_x \\ M_y \\ M_{yx} \end{Bmatrix} = \sum_{k=1}^{L} \int_{z_k}^{z_{k+1}} \begin{Bmatrix} \sigma_x \\ \sigma_y \\ \tau_{xy} \end{Bmatrix}^k z dz = \begin{bmatrix} D_{11} & D_{12} & D_{16} \\ D_{12} & D_{22} & D_{26} \\ D_{16} & D_{26} & D_{66} \end{bmatrix} \begin{Bmatrix} \phi_{x,x} \\ \phi_{y,y} \\ \phi_{x,y} + \phi_{y,x} \end{Bmatrix} \tag{4}$$

$$\begin{Bmatrix} Q_x \\ Q_y \end{Bmatrix} = K_s \sum_{k=1}^{L} \int_{z_k}^{z_{k+1}} \begin{Bmatrix} \tau_{xz} \\ \tau_{yz} \end{Bmatrix}^k dz = \begin{bmatrix} A_{55} & A_{45} \\ A_{45} & A_{44} \end{bmatrix} \begin{Bmatrix} \phi_x + w,_x \\ \phi_y + w,_y \end{Bmatrix} \tag{5}$$

where K_s is the shear correction factor.

By taking the first variation of the total potential of the plate [17], we obtain the equations of motion of the plate in terms of the stress resultants

$$\frac{\partial M_x}{\partial x} - \frac{\partial M_{xy}}{\partial y} - Q_x = I_2 \ddot{\phi}_x \tag{6a}$$

$$\frac{\partial M_{yx}}{\partial x} + \frac{\partial M_y}{\partial y} - Q_y = I_2 \ddot{\phi}_y \tag{6b}$$

$$\frac{\partial Q_x}{\partial x} + \frac{\partial Q_y}{\partial y} = I_1 \ddot{w} \tag{6c}$$

where I_1, I_2

$$I_1 = \int_{-h/2}^{h/2} \rho(z) dz, \quad I_2 = \int_{-h/2}^{h/2} z^2 \rho(z) dz \tag{7a,b}$$

with $\rho(z)$ being the density variation through the thickness. Note that the twisting moments M_{xy}, M_{yx} are positive when they have the direction of the outward normal to the cross section [17].

The associated boundary and initial conditions are:

$$\alpha_1 w + \alpha_2 Q_n = \alpha_3 \tag{8a}$$

$$\beta_1 \phi_n + \beta_2 M_n = \beta_3 \tag{8b}$$

$$\gamma_1 \phi_t + \gamma_2 M_{nt} = \gamma_3 \tag{8c}$$

$$w(x, y, 0) = g_1^{(1)}(x, y), \quad \dot{w}(x, y, 0) = g_2^{(1)}(x, y) \tag{8d}$$

$$\phi_x(x, y, 0) = g_1^{(2)}(x, y), \quad \dot{\phi}_x(x, y, 0) = g_2^{(2)}(x, y) \tag{8e}$$

$$\phi_y(x, y, 0) = g_1^{(3)}(x, y), \quad \dot{\phi}_y(x, y, 0) = g_2^{(3)}(x, y) \tag{8f}$$

where

$$Q_n = Q_x n_x + Q_y n_y, \quad M_n = M_x n_x^2 + M_y n_y^2 + 2 n_x n_y M_{yx} \tag{9a,b}$$

$$M_{nt} = M_{xy}(n_x^2 - n_y^2) + n_x n_y (M_x - M_y) \tag{9c}$$

$$\phi_n = n_x \phi_x + n_y \phi_y, \quad \phi_t = -n_y \phi_x + n_x \phi_y \tag{9d,e}$$

with n_x and n_y being the direction cosines of the normal to the boundary (Fig. 1). It is not necessary to specify the functions $g_1^{(i)}(x, y)$, $g_2^{(i)}(x, y)$, $(i = 1, 2, 3)$ of the initial conditions Eq. (8d), (8e), (8f), since we are interested on the evaluation of the natural frequencies of the plate.

All types of boundary conditions can be derived from Eqs. (8a), (8b), (8c) by appropriate selection of the parameters α_i, β_i, γ_i $(i = 1, 2, 3)$. Thus an edge is:

(i) clamped for $\alpha_1 = \beta_1 = \gamma_1 = 1$ and $\alpha_2 = \beta_2 = \gamma_2 = 0$, $\alpha_3 = \beta_3 = \gamma_3 = 0$
(ii) simply supported of type I (hard) for $\alpha_1 = \beta_2 = \gamma_1 = 1$ and $\alpha_2 = \beta_1 = \gamma_2 = \alpha_3 = \beta_3 = \gamma_3 = 0$,
(iii) simply supported of type II (soft) for $\alpha_1 = \beta_2 = \gamma_2 = 1$ and $\alpha_2 = \beta_1 = \gamma_1 = \alpha_3 = \beta_3 = \gamma_3 = 0$
(iv) free for $\alpha_2 = \beta_2 = \gamma_2 = 1$ and $\alpha_1 = \beta_1 = \gamma_1 = \alpha_3 = \beta_3 = \gamma_3 = 0$.

Substituting Eqs. (4) and (5) in Eq. (6) we obtain the equations of motion in terms of the displacements

$$\begin{aligned} &D_{11}\phi_{x,xx} + 2D_{16}\phi_{x,xy} + D_{66}\phi_{x,yy} + D_{16}\phi_{y,xx} + (D_{12} + D_{66})\phi_{y,xy} \\ &+ D_{26}\phi_{y,yy} - A_{55}(\phi_x + w_{,x}) - A_{45}(\phi_y + w_{,y}) = I_2 \ddot{\phi}_x \end{aligned} \tag{10a}$$

$$\begin{aligned} &D_{66}\phi_{y,xx} + 2D_{26}\phi_{y,xy} + D_{22}\phi_{y,yy} + D_{16}\phi_{x,xx} + (D_{12} + D_{66})\phi_{x,xy} \\ &+ D_{26}\phi_{x,yy} - A_{45}(\phi_x + w_{,x}) - A_{44}(\phi_y + w_{,y}) = I_2 \ddot{\phi}_y \end{aligned} \tag{10b}$$

$$A_{55}(\phi_{x,x} + w_{xx}) + A_{45}(\phi_{x,y} + \phi_{y,x} + 2w_{xy}) - A_{44}(\phi_{y,y} + w_{,yy}) = I_1 \ddot{w} \tag{10c}$$

2.3 Evaluation of the Objective Function

The initial-boundary value problem of Eqs. (8) and (10) is solved using the AEM [17]. Since the governing Eq. (11) represents a system of three coupled second order PDEs with respect to spatial coordinates, the analog equations are:

$$\nabla^2 w = b_1(x, y, t), \quad \nabla^2 \phi_x = b_2(x, y, t), \quad \nabla^2 \phi_y = b_3(x, y, t) \qquad (11a, b, c)$$

where b_1, b_2 and b_3 are time dependent fictitious sources, unknown in the first instance. Equations (11a,b,c) are quasi-static equations, that is the time appears as a parameter, or in other words the equations are instantaneous elliptic. Their solution is given in integral form as [18]

$$\varepsilon w(\mathbf{x}, t) = \int_\Omega u^* b_1(\mathbf{y}) d\Omega_\mathbf{y} - \int_\Gamma (u^* w_{,n} - u^*_{,n} w) ds_\xi \qquad (12a)$$

$$\varepsilon \phi_x(\mathbf{x}, t) = \int_\Omega u^* b_2(\mathbf{y}) d\Omega_\mathbf{y} - \int_\Gamma (u^* \phi_{x,n} - u^*_{,n} \phi_x) ds_\xi \qquad (12b)$$

$$\varepsilon \phi_y(\mathbf{x}, t) = \int_\Omega u^* b_3(\mathbf{y}) d\Omega_\mathbf{y} - \int_\Gamma (u^* \phi_{y,n} - u^*_{,n} \phi_y) ds_\xi \qquad (12c)$$

in which $\mathbf{x} \in \Omega \cup \Gamma$, $\mathbf{y} \in \Omega$, $\xi \in \Gamma$; $u^* = \ln r/2\pi$ is the fundamental solution of the Poisson's equation, i.e., Eq. (11a); $r = \|\mathbf{y} - \mathbf{x}\|$ in domain integrals and $r = \|\xi - \mathbf{x}\|$ in boundary integrals; ε is the free term coefficient ($\varepsilon = 1$ if $\mathbf{x} \in \Omega$, $\varepsilon = a/2\pi$ if $\mathbf{x} \in \Gamma$and $\varepsilon = 0$ if $\mathbf{x} \notin \Omega \cup \Gamma$; a is the interior angle between the tangents of boundary at point $\mathbf{x}$; $\varepsilon = 1/2$ for points where the boundary is smooth (Fig. 2a)). The subscript in the differentials, i.e., $d\Omega_\mathbf{y}$ and ds_ξ, denotes the point with respect to which the integration is performed. Eq. (12) are solved numerically using the BEM. The boundary integrals are approximated using N constant boundary elements, whereas the domain integrals are approximated using linear triangular elements resulting in total M domain nodal points (Fig. 2b). The domain discretization is performed automatically using the Delaunay triangulation. Since the fictitious source is not defined on the boundary, the nodal points of the triangles adjacent to the boundary are not placed on the vertices of the tringle but on their sides (Fig. 2c). A detailed description of integration procedure is found in [17].

Thus, after discretization and application of Eqs. (12a)–(12c) at the N boundary nodal points we obtain

$$\mathbf{H} \begin{Bmatrix} \mathbf{w} \\ \phi_x \\ \phi_y \end{Bmatrix} + \mathbf{A} \begin{Bmatrix} \mathbf{b_1} \\ \mathbf{b_2} \\ \mathbf{b_3} \end{Bmatrix} = \mathbf{G} \begin{Bmatrix} \mathbf{w_{,n}} \\ \phi_{\mathbf{x},\mathbf{n}} \\ \phi_{\mathbf{y},\mathbf{n}} \end{Bmatrix} \qquad (13)$$

where $\mathbf{H}$, $\mathbf{G}$ are $3N \times 3N$ known matrices originating from the integration of the kernel functions on the boundary elements and $\mathbf{A}$ is an $3N \times 3M$ coefficient matrix

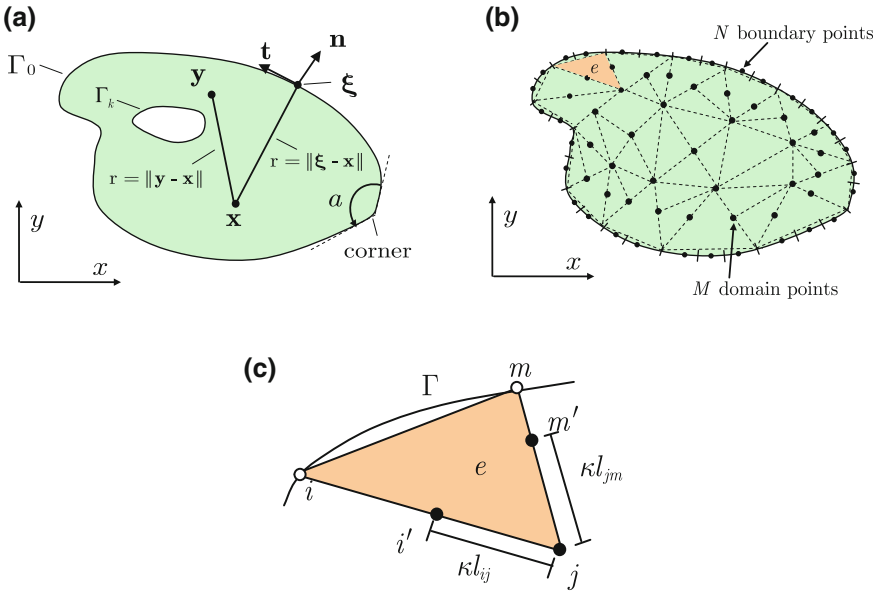

Fig. 2 **a** BEM notation; **b** boundary and domain discretization; **c** triangle adjacent to the boundary (l_{jm}, l_{im} side lengths, $0 < \kappa < 1$)

originating from the integration of the kernel function on the domain elements; $\mathbf{b}_1(t)$, $\mathbf{b}_2(t)$, $\mathbf{b}_3(t)$ are vectors containing the values of the fictitious loads at the M domain points at instant t. Applying the boundary conditions, Eqs. (8a), (8b), (8c), at the N boundary nodal points and using Eqs. (9d,e) we obtain

$$\bar{\mathbf{H}} \begin{Bmatrix} \mathbf{w} \\ \phi_x \\ \phi_y \end{Bmatrix} + \bar{\mathbf{G}} \begin{Bmatrix} \mathbf{w}_{,\mathbf{n}} \\ \phi_{\mathbf{x},\mathbf{n}} \\ \phi_{\mathbf{y},\mathbf{n}} \end{Bmatrix} = \begin{Bmatrix} \alpha_3 \\ \beta_3 \\ \gamma_3 \end{Bmatrix} \tag{14}$$

The tangential derivatives of $\phi_{x,t}, \phi_{y,t}$, which appear in the boundary conditions, are expressed in terms of ϕ_x, ϕ_y using a finite difference scheme. Equations (13) and (14) constitute a system of $6N$ algebraic equations which can be solved for the boundary quantities $w, \phi_x, \phi_y, w_{,n}, \phi_{x,n}, \phi_{y,n}$. Substituting the boundary quantities in the discretized counterpart of Eqs. (12) we obtain the displacements w, ϕ_x, ϕ_y and their derivatives at the M domain nodal points in terms of the fictitious loads

$$\mathbf{w}_{,pq}(t) = \mathbf{W}^{(1)}_{,pq}\mathbf{b}_1(t) + \mathbf{W}^{(2)}_{,pq}\mathbf{b}_2(t) + \mathbf{W}^{(3)}_{,pq}\mathbf{b}_3(t) \tag{15a}$$

$$\phi_{x,pq}(t) = \mathbf{S}^{(1)}_{,pq}\mathbf{b}_1(t) + \mathbf{S}^{(2)}_{,pq}\mathbf{b}_2(t) + \mathbf{S}^{(3)}_{,pq}\mathbf{b}_3(t) \tag{15b}$$

$$\phi_{y,pq}(t) = \mathbf{V}^{(1)}_{,pq}\mathbf{b}_1(t) + \mathbf{V}^{(2)}_{,pq}\mathbf{b}_2(t) + \mathbf{V}^{(3)}_{,pq}\mathbf{b}_3(t) \tag{15c}$$

where $p, q = 0, x, y$ and $\mathbf{W}^{(i)}_{,pq}, \mathbf{S}^{(i)}_{,pq}, \mathbf{V}^{(i)}_{,pq}$ $(i = 1, 2, 3)$ are $M \times M$ known matrices. Finally, collocating the governing Eqs. (10a), (10b), (10c) at the M domain nodal points and substituting the displacements and their derivatives from Eqs. (15), we obtain the equations of motion in terms of the fictitious loads $\mathbf{b}_1, \mathbf{b}_2, \mathbf{b}_3$

$$\mathbf{M}\ddot{\mathbf{a}} + \mathbf{K}\mathbf{a} = \mathbf{0} \tag{16}$$

where $\mathbf{M}, \mathbf{K}$ are the $3M \times 3M$ mass matrix and stiffness matrix, respectively; $\mathbf{a} = \left\{ \mathbf{b}_1 \ \mathbf{b}_2 \ \mathbf{b}_3 \right\}^T$ is a $3M \times 1$ vector with the values of the fictitious loads at instant t.

In order to evaluate the natural frequencies of the plate we assume a time harmonic solution

$$\mathbf{a}(t) = \beta e^{i\omega t} \tag{17}$$

where β is a vector of time independent parameters and ω the frequency of the vibration. Substituting Eq. (17) in (16) we obtain

$$\left(-\omega^2 \mathbf{M} + \mathbf{K}\right) \ \beta = 0 \tag{18}$$

Equation (18) is an eigenvalue problem which is solved numerically by ready to use program (Matlab function). The first eigenfrequency is the objective function of the optimization problem.

2.4 The Optimization Procedure

The frequency optimization problem reads:

$$\text{maximize } \omega_1 \text{ or minimize } \omega_1 \text{ or minimize } (1 - \omega_1/\omega_{pr})^2 \tag{19}$$

under the constraints of lower θ_l and upper θ_u bounds

$$\theta_l < \theta_k < \theta_u \tag{20}$$

where $\omega_1 = \omega_1(\theta_1, \theta_2, ..., \theta_k)$ is the fundamental frequency of the plate and ω_{pr} a prescribed value between the bounds.

The optimization problem is solved with the sequential quadratic programming (SQP) algorithm using Matlab function *fmincon*. This method belongs to the classical gradient based methods. The optimum solution is regarded as a local optimum. The global optimum can be obtained by exhaustive search of the design space starting the optimization procedure from various initial solutions.

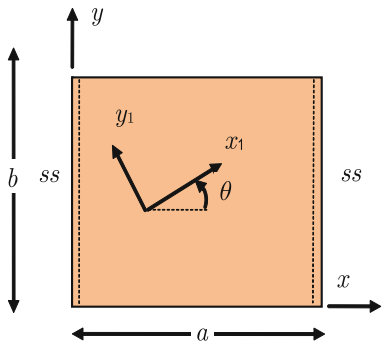

Fig. 3 Rectangular laminated plate of Example 1

3 Examples

Example 1 As a first example we optimize a rectangular $a \times b$ laminated plate with thickness $h = 0.1a$ made of two layers of orthotropic material with stacking sequence $(\theta, -\theta)$. The material parameters are: $E_1 = 132.38$GPa, $E_2 = 10.76$GPa, $G_{12} = G_{13} = 5.65$GPa, $G_{23} = 3.61$GPa, $\nu_{12} = 0.25$. The plate is simply supported (type I) along the sides $x = 0, a$ while various types of boundary conditions are considered for the sides $y = 0, b$, more specifically (Fig. 3):

(i) simply supported at $y = 0, b$;
(ii) clamped at $y = 0$ and simply supported at $y = b$
(iii) clamped at $y = 0, b$
(iv) free at $y = 0$ and simply supported at $y = b$
(v) free at $y = 0$ and clamped at $y = b$

The results were obtained using $N = 200$ boundary elements and $M = 181$ domain points resulting from 300 triangular elements (Fig. 4). Figure 5 presents the non-dimensional fundamental frequency $\bar{\omega}_1 = \omega_1 a\sqrt{\rho/E_2 h^2}$ versus angle θ for the different boundary conditions of the analyzed square plate. The results are compared with those obtained by Levy-type solution [20] for three angles, i.e., $\theta = 30, 45, 60$. Table 1 presents the optimum value of angle θ for maximum fundamental frequency for the considered types of boundary conditions of the square plate. Finally, Fig. 6 presents optimum angle θ for maximum fundamental frequency versus aspect ratio a/b for three different boundary conditions. It is observed that the optimum ply orientation of each lamina tends to be parallel to one of the plate sides as the aspect ratio increases. Note the notation for the opposite sides: ss = both simply supported; cc = both clamped; cs = clamped-simply supported; fs = free-simply supported; fc = free-clamped.

Example 2 A rectangular thick laminated plate $a \times b$ consisting of four layers of equal thickness made of orthotropic material is optimized. The elastic parameters are: $E_1 = 40E_2$, $G_{12} = G_{13} = 0.6E_2$, $G_{23} = 0.5E_2$, $\nu_{12} = 0.25$, $E_2 = 1$GPa. The plate is simply supported (type I) along the boundary. The total thickness

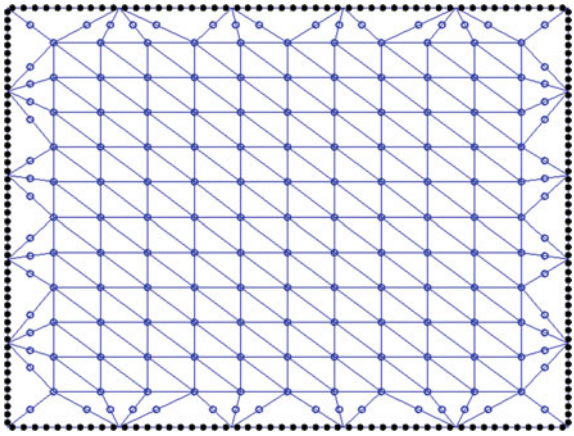

Fig. 4 Boundary and domain discretization of rectangular plate in Example 1

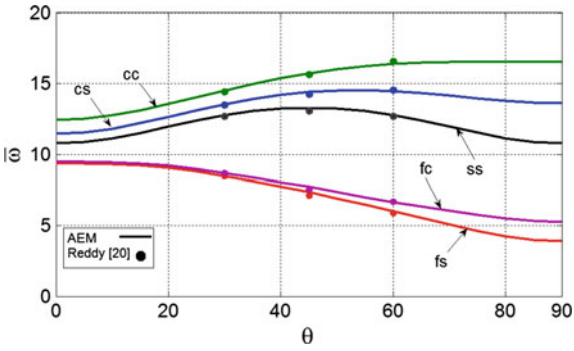

Fig. 5 Frequency $\bar{\omega}_1$ versus angle θ $(0 \leq \theta \leq 90)$ for the various cases of the boundary conditions in Example 1

Table 1 Optimum angle θ for maximum fundamental frequency in Example 1

Boundary condition	ss	cs	cc	fs	fc
$\theta_{optimum}$	45	55	75	0	0
$\bar{\omega}_{1max}$	13.27	14.53	16.54	9.35	9.46

of the plate is $h = 0.1a$. Two cases of stacking sequence are studied: symmetric $(\theta_1, \theta_2, \theta_2, \theta_1)$ and antisymmetric $(\theta_1, \theta_2, -\theta_2, -\theta_1)$. The results were obtained using $N = 200$ boundary elements and $M = 133$ domain points resulting from 212 triangular elements. Figures 7 and 8 present the non-dimensional fundamental frequency $\bar{\omega}_1 = \omega_a \sqrt{\rho / E_2 h^2}$ versus angles θ_1 and θ_2 for symmetric and antisymmetric laminates for the square $(a = b)$ and a rectangular plate $(b = a/2)$, respectively. It is observed that there are various local optimum solutions for a maximum or minimum fundamental frequency. Tables 2 and 3 present the optimum angles θ_1 and θ_2 for maximum fundamental frequency, starting from different initial values of the

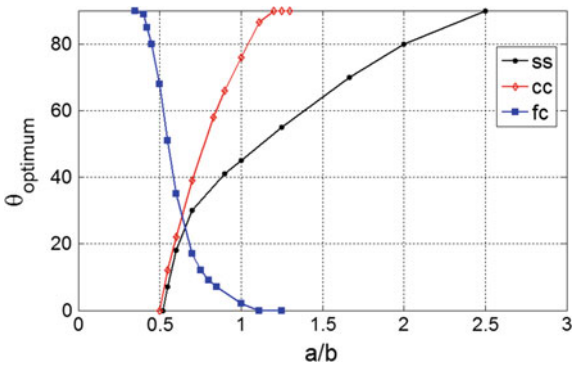

Fig. 6 Optimum angle θ versus aspect ratio a/b for three different boundary conditions in Example 1

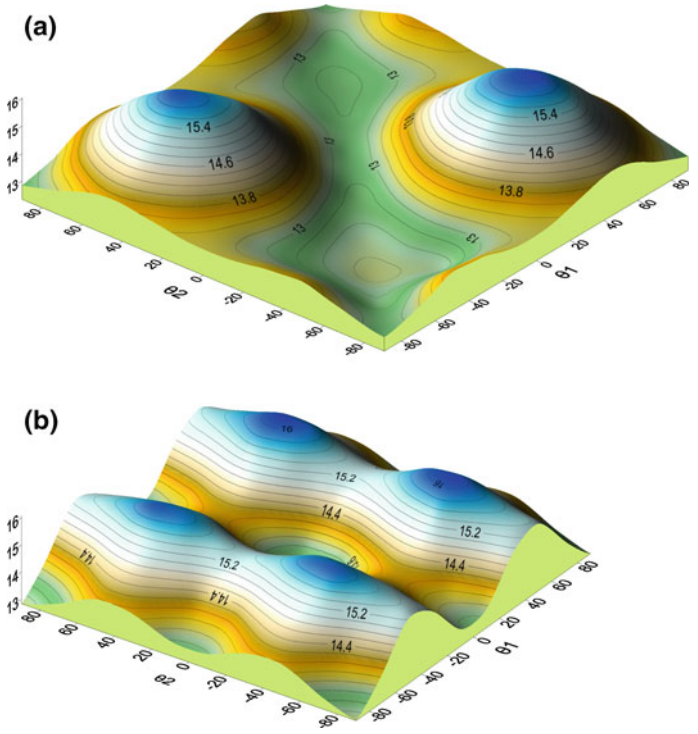

Fig. 7 Frequency $\bar{\omega}_1$ versus angle θ_1 and θ_2 for **a** symmetric and **b** antisymmetric square plate in Example 2

design variables. Finally, Tables 4 and 5 present local optimum sets of θ_1 and θ_2 for minimum fundamental frequency.

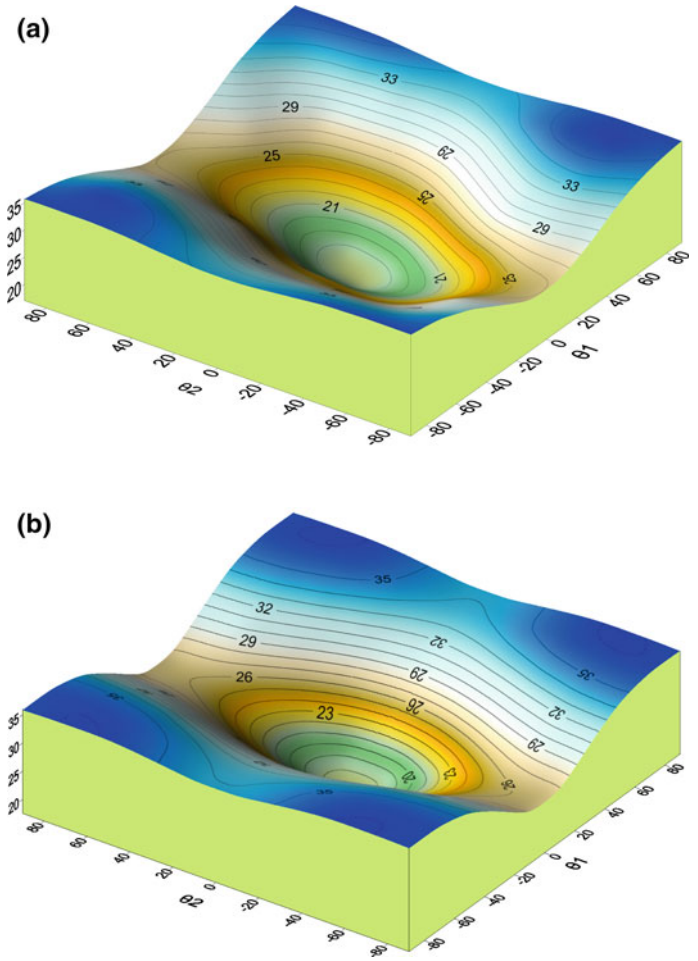

Fig. 8 Frequency $\bar{\omega}_1$ versus angles θ_1 and θ_2 for **a** symmetric and **b** antisymmetric rectangular plate $a \times (a/2)$ in Example 2

Example 3 The laminated cantilever plate of Fig. 9a simulating an airplane wing is optimized. The plate consists of 5 layers with total thickness $h = 0.2$ m (Fig. 9b). The face sheets (layers 1 and 5) are made of isotropic material with elastic parameters $E = 70$ GPa, $\nu = 0.333$, mass density $\rho = 2.7\,\text{kNs}^2/\text{m}^{-4}$ and thickness $h_s = 0.01$ m. The core with thickness $h_c = 0.18$ m consists of three layers of equal thickness made of orthotropic material in sequence $(\theta_1, \theta_2, \theta_3)$ with elastic parameters $E_1 = 25E_2$, $G_{12} = G_{13} = 0.5E_2$, $G_{23} = 0.2E_2$, $E_2 = 10$ GPa, $\nu_{12} = 0.25$ and mass density $\rho = 1.55\,\text{kNs}^2/\text{m}^{-4}$. The results were obtained with $N = 310$ boundary elements and $M = 215$ internal nodal points resulting from 350 linear triangular elements (Fig. 9c). Tables 6 and 7 present the initial and the optimum set of the design variables for the

Table 2 Optimum angles θ_1 and θ_2 for maximum fundamental frequency $\bar{\omega}_1$ of a square plate in Example 2

	Initial		Optimum		$\max \bar{\omega}_1$
	θ_1	θ_2	θ_1	θ_2	
Symmetric	−20	20	−45.19	45.10	16.24
	20	−20	44.74	−44.99	16.39
	20	20	90	45.12	14.01
	−20	−20	−90	−45.58	13.90
Antisymmetric	20	20	44.85	44.96	16.39
	−20	−20	−45.15	−45.10	16.24
	20	−20	44.80	−44.95	16.39
	−20	20	−45.15	45.10	16.24

Table 3 Optimum angles θ_1 and θ_2 for maximum fundamental frequency $\bar{\omega}_1$ of a rectangular plate $a \times a/2$ in Example 2

	Initial		Optimum		$\max \bar{\omega}_1$
	θ_1	θ_2	θ_1	θ_2	
Symmetric	60	−60	79.01	−64.08	36.31
	60	60	90.00	68.93	36.03
	−60	60	−80.40	63.72	36.45
Antisymmetric	60	60	84.21	62.74	36.37
	60	−40	84.21	62.74	36.37
	−40	−40	84.20	62.74	36.37

Table 4 Optimum angles θ_1 and θ_2 for minimum fundamental frequency $\bar{\omega}_1$ of a square plate in Example 2

	Initial		Optimum		$\min \bar{\omega}_1$
	θ_1	θ_2	θ_1	θ_2	
Symmetric	10	10	−1.01	0.01	13.11
	−60	20	−88.72	0.01	13.54
	−60	−60	−88.85	−90.00	13.11
Antisymmetric	−60	−60	−58.62	−58.35	12.98
	60	60	58.51	58.37	12.86
	60	−60	90.00	−88.89	13.11

maximum, minimum as well as for a specified value of the fundamental frequency. Figures 10 and 11 present the fundamental frequency versus θ_1, θ_2 and θ_3 (Table 8).

Table 5 Optimum angles θ_1 and θ_2 for minimum fundamental frequency $\bar{\omega}_1$ of rectangular plate $a \times a/2$ in Example 2

	Initial		Optimum		$\min \bar{\omega}_1$
	θ_1	θ_2	θ_1	θ_2	
Symmetric	20	20	−1.90	−1.90	17.18
	−60	60	−1.89	−1.90	17.18
	60	−60	−1.91	−1.92	17.18
Antisymmetric	40	40	−0.56	0.012	17.43
	40	−40	−0.56	0.012	17.43
	−60	60	−0.56	0.012	17.43

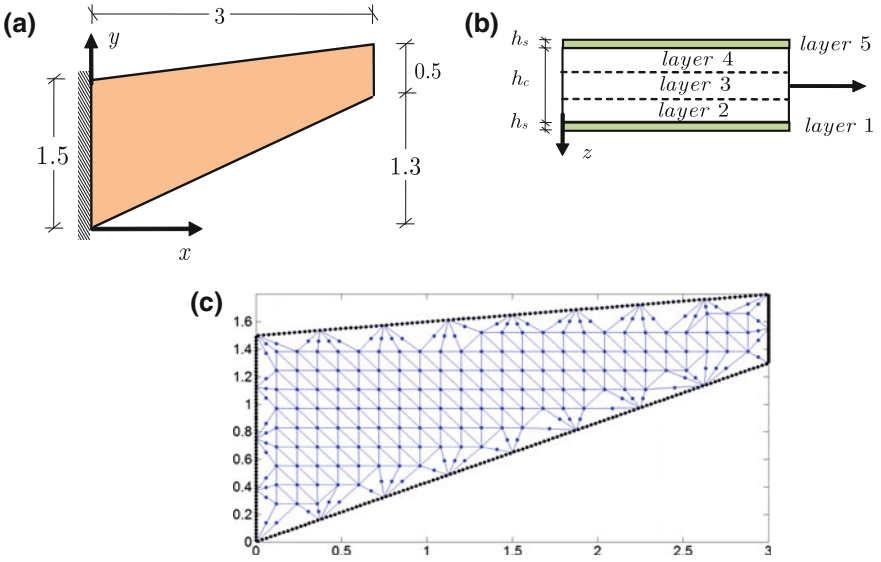

Fig. 9 **a** Geometry of cantilever plate, **b** stacking sequence and **c** boundary and domain discretization in Example 3

Table 6 Initial and optimum angles θ_1, θ_2 and θ_3 for maximum fundamental frequency ω_1 of the cantilever plate in Example 3

Initial			Optimum			$\max \omega_1$
θ_1	θ_2	θ_3	θ_1	θ_2	θ_3	
0	0	0	11.87	11.06	11.76	317.91
60	60	60	11.91	10.84	11.76	317.91
−10	−20	−10	11.93	10.81	11.74	317.91

Table 7 Initial and optimum angles θ_1, θ_2 and θ_3 for minimum fundamental frequency ω_1 of the cantilever plate in Example 3

Initial			Optimum			$\min \omega_1$
θ_1	θ_2	θ_3	θ_1	θ_2	θ_3	
0	0	0	−89.24	90	−89.94	109.92
0	−30	0	84.47	−67.64	−90.00	108.10
70	70	−20	−90	−69.63	−490	108.48

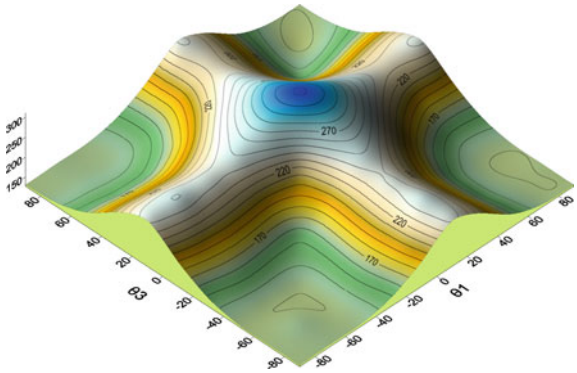

Fig. 10 Fundamental frequency versus angle θ_1 and θ_3 for $\theta_2 = 11.06^0$ in Example 3

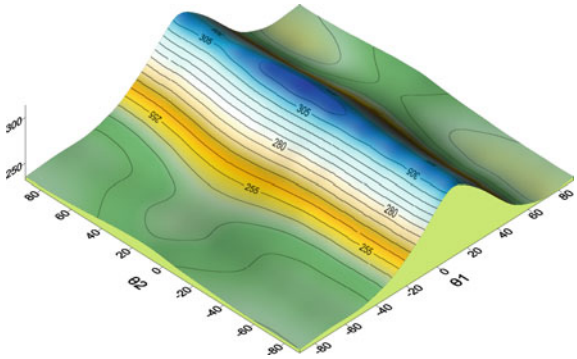

Fig. 11 Fundamental frequency versus angle θ_1 and θ_2 for $\theta_3 = 11.76^0$ in Example 3

Table 8 Initial and optimum angles θ_1, θ_2 and θ_3 for specified fundamental frequency $\omega_1 = 250$ of the cantilever plate in Example 3

Initial			Optimum			
θ_1	θ_2	θ_3	θ_1	θ_2	θ_3	
0	0	0	−9.73	4.87	−9.88	$w_1^{=}250$
20	20	0	31.50	21.25	−25.52	
20	0	20	29.54	0.90	29.54	

4 Conclusions

The problem of frequency regulation of a thick laminated plate made of various orthotropic layers is studied. The plate may have arbitrary geometry and is subjected to any type of boundary conditions. The optimization problem consists in determining the angle of the material principal direction of each layer (ply orientation) for which the plate fundamental frequency is optimized, i.e., it becomes minimum, maximum or reaches certain specified value between the extrema. The optimization problem is subjected to upper and lower bounds on ply orientation. The fundamental frequency (objective function) is evaluated by the solution of the free vibration problem of a thick anisotropic plate. This problem is described by a system of three coupled hyperbolic partial differential equations (PDE) of second order. Using the AEM the coupled PDEs are converted into three uncoupled quasi-static Poisson's equations, which are solved by the conventional BEM with constant boundary elements and linear triangular elements for domain discretization. The optimization problem is solved using sequential quadratic programming algorithm by a ready-to-use Matlab function.

Several optimization problems for plates of various shapes and boundary conditions have been analyzed, yielding realistic and meaningful optimum designs. The main conclusions of the presented investigation are:

(a) The fundamental frequency of a thick laminated plate can change considerably (more than 100%) by optimizing the ply orientation of its layers.
(b) The design space includes many local optima and requires exhaustive search, starting the optimization procedure from various initial points. Otherwise modern evolutionary methods should be included in the optimization procedure.
(c) In rectangular plates the optimum ply-orientation for maximum fundamental frequency tends to be parallel to one of its sides as the aspect ratio increases.

References

1. Narita, Y.: Layerwise optimization for the maximum fundamental frequency of laminated composite plates. J. Sound Vib. **263**, 1005–1016 (2003)
2. Yoshihiro, Narita: Maximum frequency design of laminated plates with mixed boundary conditions. Int. J. Solids Struct. **43**, 4342–4356 (2006)
3. Apalak, K.M., Yildirim, M., Ekici, R.: Layer optimization for maximum fundamental frequency of laminated composite plates for different edge conditions. Compos.Sci. Technol. **68**, 537–550 (2008)
4. Ghashochi, B.H., Sadr, M.H.: Stacking sequence optimization of composite plates for maximum fundamental frequency using particle swarm optimization algorithm. Meccanica **47**, 719–730 (2012)
5. Houmat, A.: Optimal lay-up design of variable stiffness laminated composite plates by a layerwise optimization technique. Eng. Optim. (2017). https://doi.org/10.1080/0305215X.2017.1307978
6. Pai, P.: A new look at shear correction factors and warping functions of anisotropic laminates. Int. J. Solids Struct. **32**(16), 2295–2313 (1995)

7. Fares, M.E., Youssif, Y.G., Alamir, A.E.: Optimal design and control of composite laminated plates with various boundary conditions using various plate theories. Compos. Struct. **56**, 1–12 (2002)
8. Kam, T.Y., Chang, R.R.: Design of laminated composite plates for maximum buckling load and vibration frequency. Comput. Methods Appl. Mech. Eng. **106**, 65–81 (1993)
9. Kam, T.Y., Lai, F.M.: Design of laminated composite plates for optimal dynamic characteristics using a constrained global optimization technique. Comput. Methods Appl. Mech. Eng. **120**, 389–402 (1995)
10. Topal, U., Uzman, U.: Frequency optimization of laminated folded composite plates. Mater. Design **30**, 494–501 (2009)
11. Huang, C., Kröplin, B.: On the optimization of composite laminated plates. Eng. Comput. **12**, 403–414 (1995)
12. Vo-Duy, T., Ho-Huu, V., Do-Thi, T.D., Dang-Trung, H., Nguyen-Thoi, T.: A global numerical approach for lightweight design optimization of laminated composite plates subjected to frequency constraints. Compos. Struct. **159**, 646–655 (2017)
13. Assie, A.E., Kabeel, A.M., Mahmoud, F.F.: Optimum design of laminates composite plates under dynamic excitation. Appl. Math. Modell. **36**, 668–682 (2012)
14. Vosoughi, A.R., Nikoo, M.R.: Maximum fundamental frequency and thermal buckling temperature of laminated composite plates by a new hybrid multi-objective optimization technique. Thin-Walled Struct. **95**, 408–415 (2015)
15. Vosoughi, A.R., Dehghani Forkhorji, H., Roohbakhsh, H.: Maximum fundamental frequency of thick laminated composite plates by a hybrid optimization method. Compos. Part B **86**, 254–260 (2016)
16. Topal, U., Dede, T., Tahsin Ozturk, H.: Stacking sequence optimization for maximum fundamental frequency of simply supported antisymmetric laminated composite plates using teaching-learning-based optimization. KSCE Journal of Civil Engineering **18**, 1–8 (2017)
17. Katsikadelis, J.T.: The Boundary Element Method for Plate Analysis. Academic Press, Elsevier (2014)
18. Katsikadelis, J.T.: The Boundary Element method for Engineer and Scientists. Academic Press, Elsevier (2016)
19. Mindlin, R.D.: Influence of rotary inertia and shear on flexural motions of isotropic, elastic plates, ASME. J. Appl. Mech. **18**, 31–38 (1951)
20. Reddy, J.N.: Mechanics of Laminated Composite Plates and Shells Theory and Analysis. CRC Press, Florida (2003)